

Sensitivity of Traffic Speed to Rainfall

KAUSTUBH ANIL SALVI,^a MUKESH KUMAR,^b AND ALEXANDER M. HAINEN^b

^a *Alabama Transportation Institute, University of Alabama, Tuscaloosa, Alabama*

^b *Department of Civil Construction and Environmental Engineering, University of Alabama, Tuscaloosa, Alabama*

(Manuscript received 14 February 2022, in final form 27 August 2022)

ABSTRACT: Hazardous weather conditions can pose a threat to the functioning of transportation systems. While the impacts of extreme weather events (e.g., hurricanes/tornadoes and flooding) on transportation disruptions have received significant attention, minor transient disturbances in traffic and transport systems due to rainfall events have remained understudied. Given that a road network experiences rainfall events on a regular basis, which in turn likely reduces its efficiency through short-term disruptions, it is imperative to assess the influence of variations in rainfall intensity on the traffic speed. By synergistically using crowdsourced probe vehicle speed data and spatially explicit meteorological data, this study quantifies the sensitivity of traffic speed to rainfall events of different intensities over 1151 road sections within Alabama. It is observed that instead of variations in the rainfall intensity, traffic speed sensitivity is primarily influenced by a road section's free-flow speed (uninterrupted speed during dry pavement conditions) and antecedent traffic volume. Relative sensitivity of road sections exhibits high consistency over different rainfall intensities across all road sections, thus underscoring the possibility of assessing sensitivities based only on speed data collected during rainfall intensities that are much more frequent. These results may be used to identify road sections and time periods with high sensitivity to rainfall, thus helping in prioritization of mitigation measures.

SIGNIFICANCE STATEMENT: To safeguard against hazardous driving conditions during rainfall events, from either compromised visibility or reduced friction between tires and pavement, drivers often reduce vehicle speed. However, the influence of rainfall intensity on traffic speed reduction remains unclear. This study analyzes the sensitivity of traffic speed to rainfall intensity. Our results indicate that, while rainfall indeed leads to traffic speed reductions, the extent of reduction is predominantly influenced by free-flow speed (uninterrupted vehicle speed) of the road section and the traffic volume on it instead of the rainfall intensity. These results may be used to identify high-sensitivity time periods and locations and guide prioritization of mitigation measures.


KEYWORDS: Extreme events; Rainfall; Transportation meteorology

1. Introduction

Inclement weather conditions, sometimes contributed by the changing climate (IPCC 2021; Alizadeh-Choobari and Najafi 2018; Ludlow and Travis 2019), impact the transportation system in a multitude of ways (Andrey et al. 2003; Pregnotato et al. 2017; Omranian et al. 2018). Failures in sections of the transportation network may proliferate over larger areas, with cascading negative effects (Martín et al. 2021). Major interruptions in road-based transportation by severe winter storms, hurricanes, or flooding have received significant attention (Barjenbruch et al. 2016; Pregnotato et al. 2017; Barrett et al. 2000), as their impacts may last days to weeks and cost millions of dollars. Notably, minor transient disturbances in traffic and transport systems due to rain, fog, snow, freezing rain, etc., although relatively understudied, may also play an important part in reducing the efficiency of such systems and result in increased fuel consumption, delay, and number of crashes

(Calvert and Snelder 2018; Hranac et al. 2006). Rainfall intensity, in particular, has been frequently identified to cause significant impacts on driving conditions and network performance (Prokhorchuk et al. 2021; Lam et al. 2013; Bartlett et al. 2013; Lu 2014; Souleyrette et al. 2006; Billot et al. 2009; Rakha et al. 2008), even leading to increase in crash and injury rates (Black et al. 2017). Two common repercussions of rainfall are compromised road visibility and reduction in traction due to hydroplaning. At an individual vehicle level, these challenges are tackled by reducing vehicle speed, resulting in altered network performance with respect to dry conditions. Therefore, understanding the effect of rainfall on traffic speed is extremely important to identify hot spots that are markedly influenced by rainfall.

Here, we assess the response of traffic speed to rainfall events. While several studies have evaluated the performance of transportation networks in terms of the threshold forcing the network can withstand without deviating from the usual performance or the capacity to recover after inclement weather conditions (Sarlus et al. 2020; Ortega et al. 2020; Jenelius et al. 2006; Valenzuela et al. 2017; Pregnotato et al. 2017; Abdulla et al. 2020; Nogal et al. 2017; Ganin et al. 2017; Gauthier et al. 2018; Han and Zhang 2020; Mathew and Pulugurtha 2022), it remains unclear how the traffic speed varies with rainfall intensity and what are the ancillary controls on this

 Supplemental information related to this paper is available at the Journals Online website: <https://doi.org/10.1175/WCAS-D-22-0024.s1>.

Corresponding author: Mukesh Kumar, mkumar4@eng.ua.edu

DOI: 10.1175/WCAS-D-22-0024.1

© 2022 American Meteorological Society. For information regarding reuse of this content and general copyright information, consult the [AMS Copyright Policy](#) (www.ametsoc.org/PUBSReuseLicenses).

variation. To address this need, we quantify the sensitivity or the reduction in traffic speed with respect to a reference speed vis-à-vis rainfall intensity. We further assess this sensitivity with respect to the free-flow speed of the road section and diurnal and within-week traffic volume variations. Last, we evaluate the consistency of speed sensitivity of the road network across a range of rainfall intensities. The study is carried out over more than 1000 road sections [covering 717.55 mi (1 mi \approx 1.61 km) of freeways] within Alabama. Alabama receives relatively high average rainfall [50–55 in. (1 in. \approx 2.54 cm)] within a year (Cope et al. 1962; Sen et al. 2010), which offers ample opportunity to understand the traffic speed response to rainfall. Organization of the paper is as follows. Sections 2 and 3 describe the data and method adopted in this study. Results and discussions are presented and discussed in section 4. Section 5 details the summary and conclusions.

2. Data

To obtain the sensitivity of road sections, data of vehicle speed and meteorological forcing encountered by the road section are needed. The vehicle speed data are obtained from a commercially available crowdsourced probe vehicle dataset and meteorological data are derived from the North American Land Data Assimilation System (NLDAS).

a. Crowdsourced speed data

One of the major data sources of real-time traffic information is crowdsourced probe vehicle speed data (https://www.fhwa.dot.gov/innovation/everydaycounts/edc_6/crowdsourcing.cfm). It is a commercial link-based speed dataset collected mainly from probe vehicles (Bae et al. 2018). For this study, we used crowdsourced probe vehicle data by HERE Technologies (<https://www.here.com/>). The data provide real-time and historical traffic information. Even though the data have a wide applicability in understanding different aspects of existing traffic network system and in decision-making, a full-fledged validation of the data against the ground realities is still in progress. Validation performed by Verendel and Yeh (2019) over selected roads in a Swedish city revealed that crowdsourced probe vehicle data are able to capture anomalies in travel speed, even though they sometimes miss instantaneous high speeds. Based on this and current guidance from the U.S. Federal Highway Administration, the data are considered to be appropriate for traffic sensitivity analysis that relies on capture of drop in speed during rain events.

b. NLDAS data

Climate data from the NLDAS project (Cosgrove et al. 2003) are used. The data are result of a collaborative endeavor of NOAA/NCEP's Environmental Modeling Center (EMC), NASA GSFC's Hydrological Sciences Laboratory, Princeton University, the University of Washington, the NOAA/NWS Office of Hydrological Development (OHD), and the NOAA/NCEP Climate Prediction Center (CPC). These data, consisting of 10 climate variables, are available at 0.125° spatial and an hourly temporal resolution and have been widely used in a range of disciplines such as hydrology

(Pan et al. 2003; Schaake et al. 2004; Sitterson et al. 2020; Xia et al. 2012; Xu et al. 2018; Zhang et al. 2020; Chen et al. 2020), public health (Al-Hamdan et al. 2014), and agriculture (Lewis et al. 2014). In this study, precipitation and temperature data are the two climate variables from the NLDAS product used to quantify and characterize rainfall or liquid precipitation events. As the precipitation data may consist of snow events or events with a combination of snow and rain, in order to separate and extract liquid phase (i.e., rainfall from the precipitation data), a temperature-based filter is applied (Auer 1974; Dai 2008). Although, there is a fair amount of uncertainty associated with the temperature threshold as different methods (Auer 1974; Dai 2008; Marks et al. 2013; Jennings et al. 2018) point to different temperature values associated with rainfall versus snowfall, it is recognized that precipitation events during which the temperature is greater than 4°C are highly likely to fall as rain (Dai 2008). Here we use this conservative temperature threshold ($>4^{\circ}\text{C}$) to ensure that the events selected are rainfall events.

3. Method

Response of traffic speed to rainfall events is quantified using a series of steps. First, road sections of interest are selected. This is followed by mapping of climate and vehicle speed data, which are at different spatiotemporal resolutions, onto the selected road sections. A reference speed matrix depicting average speed of vehicles in each hour of the day and on different days of week is also generated for each road section. Last, a sensitivity metric is obtained. More details are presented below.

a. Selection of road sections

Within the crowdsourced probe vehicle data, road sections are of varying lengths ranging from 0.1 to \sim 5 mi and are referred to as traffic message channels (TMCs). Average speed of a sample fraction of vehicles within each TMC (identified by a unique TMC ID) is recorded every minute (reported with time stamp). Along with this, the database also provides the free-flow speed (FFS), which indicates the speed on the road segment at which vehicles are considered to be able to travel without impediment. It is calculated as the 80th percentile of observed speeds during nonrush hours, and hence FFS is a constant value for a given TMC (similar to a speed limit). The details of these calculations have not been provided by the crowdsourced probe vehicle data. However, this approach is similar to the “engineering study method” of establishing speed limit, where speed limits are set near the 85th-percentile speed (Hosseini et al. 2015). In other words, FFS can be considered as a surrogate for speed limits. A confidence descriptor (ranging from 0 to 1) associated with each speed record is also reported in the crowdsourced probe data. A confidence magnitude above 0.7 indicates that the reported vehicle speed data were observed, and a confidence value of less than 0.7 indicates that the reported data have been filled using statistical algorithms. Here we only selected the time steps with confidence greater than 0.75. While data pertaining to \sim 10000 TMCs from all over Alabama are available in the

database, for computational feasibility and to satisfy constraints set by the data custodian, a smaller sample set is selected. Selection of the sample size is guided by 1) the level of precision (sampling error) desired, 2) confidence level provided by the sample, and 3) the degree of variability (Israel 1992). A conservative estimate of sample size for population equal to $\sim 10,000$ with a precision level equal to $\pm 3\%$, confidence level of 95%, and degree of variability equal to 0.5 is 1000 (Israel 1992). So, for the current study, a minimum sample size of 1000 is targeted. While selecting TMCs, an additional precaution is taken to make sure that TMCs 1) belong to different speed classes and experience a range of precipitation regimes [to this end, it was also desirable that each selected TMC encountered at least three rainfall events belonging to the different rainfall intensity classes considered in this study (explained in section 3e)] and 2) are spatially distributed (Fig. S1 in the online supplemental material) so as to cover varied precipitation regimes and driver behavior across Alabama. Eventually, 1151 TMCs are selected. Sensitivity calculation for each TMC is carried out next. Subsequent sections provide detailed information about the procedure adopted to quantify the sensitivity of a given TMC (Fig. 1). The same procedure is repeated for 1151 TMCs to obtain sensitivity metrics.

b. Spatiotemporal mapping of climate and speed data

The climate data (i.e., precipitation and temperature) from the NLDAS project that are used in this study are available at a spatial resolution of $1/8^\circ$ ($\sim 13 \text{ km} \times 13 \text{ km}$ in Alabama) and an hourly temporal resolution. The vehicle speed data, on the other hand, are available for each TMCs at temporal resolution of a minute. To map precipitation and temperature data to a given TMC, data are extracted from NLDAS dataset by identifying the NLDAS grid encompassing the selected TMC (Fig. 1a). The overlapping operation is carried out within ArcMap 10.6.1. The crowdsourced probe vehicle data stored at 1-min resolution are then mapped to the hourly NLDAS data. For example, between 1000 and 1100 local time (LT; Fig. 1a), an NLDAS grid will have a single value of temperature and precipitation. However, for the same duration, there are 60 observations (one for every minute) of vehicle speed (and other fields such as time stamp and confidence) from crowdsourced probe vehicle data. Because the ensuing analysis is carried out at hourly temporal resolution, the 60 observations are used to obtain a single sensitivity value for each hour (discussed in section 3d). The time period selected for the sensitivity analysis is from May 2018 to December 2018. This is because for 2018 the speed data for most of the TMCs ($>90\%$) start from May.

c. Reference speed

Reference speed in the context of this study is defined as the estimated average speed of vehicles during dry pavement conditions. It is to be noted that this term is different from the FFS, which is a single value (speed at which vehicle can travel on the TMC that is free from impediments). To obtain the reference speeds for dry pavement conditions, a matrix with

7 rows (one for each day) and 24 columns (for 24 h) (Fig. 1b) is generated. To this end, speed data for a given day-hour combination (e.g., Thursday, 1000 LT) during which dry pavement conditions exist, are averaged. The dry pavement conditions are assumed to be prevalent when rainfall for that hour is equal to zero and temperature is greater than 4°C . It is to be noted that the aforementioned weather conditions may not always ensure a dry pavement, and that may introduce errors in estimates of reference speed. For example, some water may be retained on the pavement because of rainfall during the previous hours, or temporary water leakage from a nearby water source may also lead to wet pavements. Accurate assessment of whether a pavement is wet or not may be alternatively obtained through implementation of spatially explicit hydrologic models; however, the approach is expected to be affected by inherent model-structure and parameter uncertainties as well (Beven 1993). Fortunately, the errors introduced in estimation of reference speed due to misclassification of a wet pavement as dry are expected to get smaller with longer term data. To further assess the robustness of results, we performed an additional reference speed calculation wherein a dry pavement is assumed to be prevalent when rainfall is equal to zero and temperature is greater than 4°C both in the current and the last hour.

d. Sensitivity calculations

Response of road traffic to a rainfall event is usually realized in form of reduction in speed. The speed can be tracked using the crowdsourced probe data, which are available at a 1-min resolution; that is, for any given hour there are 60 speed values. Subtracting these 60 values from the reference speed yields 60 speed anomalies. Maximum anomaly during an hour with rainfall occurrence, that is, hours during which precipitation is greater than zero and temperature is more than 4°C , is termed as sensitivity of the TMC for that hour (see Fig. 1c). Representing the sensitivity of TMC using the maximum anomaly allows capturing the transience of vehicle speed variations in response to short-burst rainfall events during an hour. To obtain sensitivity of a TMC for a given rain intensity, the average of maximum anomaly encountered over hours with the concerned rainfall intensity is evaluated. The procedure is repeated for all the TMCs chosen in this study.

e. Rainfall and speed classes

Sensitivity evaluation is then performed for four rain classes that encompass the full range of rainfall intensities existent in Alabama. The considered rainfall classes are 1) $>0\text{--}2.5$, 2) $2.5\text{--}5$, 3) $5\text{--}7.5$, and 4) $>7.5 \text{ mm h}^{-1}$. While selecting these ranges, it was confirmed that each TMC has encountered at least three rainfall events belonging to the mentioned intensities. Sensitivity assessment is also performed for 10 different ranges of FFSs, that is, the speed with which vehicles are able to travel without an exogenous impediment. As discussed in section 3a, since FFSs act as surrogates of the speed limit, these are used as a basis to categorize TMCs into different classes. The speed classes include 1) speed class 25 mi h^{-1} (hereinafter mph; $1 \text{ mph} \approx 1.61 \text{ km h}^{-1}$); FFS $22.5\text{--}27.5 \text{ mph}$,

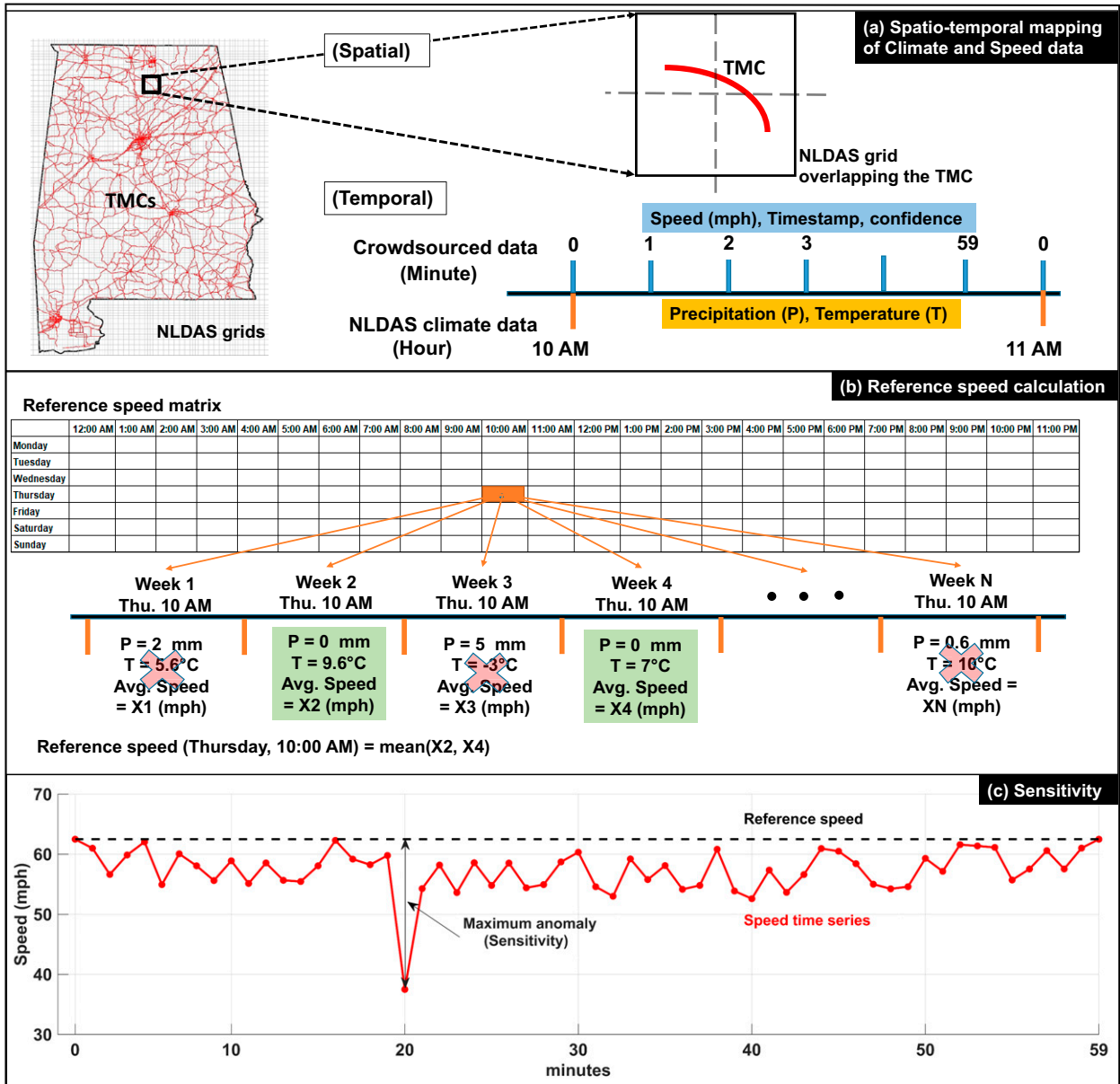


FIG. 1. Multistep method for calculating traffic speed sensitivity of a road section to rainfall event. Each road section is identified as a unique traffic message channel. (a) For each TMC, first, a spatiotemporal mapping of climate and crowdsourced speed data is performed. (b) Next, a reference speed matrix is obtained for each TMC. The reference speed estimate for a given day–hour combination only considers data of periods when the pavement is dry and the data confidence identifier is >0.75. In the example above, of *N* data periods, only two (viz., X2 and X4) satisfy these criteria. (c) Last, sensitivity is calculated for a given TMC for each rainfall event by subtracting all speed data from the reference speed and identifying the maximum anomaly for that given hour.

2) speed class 30 mph: FFS 27.5–32.5 mph, 3) speed class 35 mph: FFS 32.5–37.5 mph, 4) speed class 40 mph: FFS 37.5–42.5 mph, 5) speed class 45 mph: FFS 42.5–47.5 mph, 6) speed class 50 mph: FFS 47.5–52.5 mph, 7) speed class 55 mph: FFS 52.5–57.5 mph, 8) speed class 60 mph: FFS 57.5–62.5 mph, 9) speed class 65 mph: FFS 62.5–67.5 mph, and 10) speed class 70 mph: FFS 67.5–72.5 mph. Notably, the speed data obtained from the crowdsourced database are expressed in miles per hour. In addition, the Federal Highway Administration (FHWA), a

division of the United States Department of Transportation, also specifies all speed limits in miles per hour. To be consistent, the ensuing analysis also uses the same unit. The speed classes mentioned here are decided on the basis of commonly observed speed limits for roads within Alabama as per Highway Performance Monitoring System (HPMS) (e.g., Islam et al. 2021). Ideally, marked speed limit could have been used to define speed classes, however, crowdsourced probe data do not provide speed limits, and HPMS speed limit data for

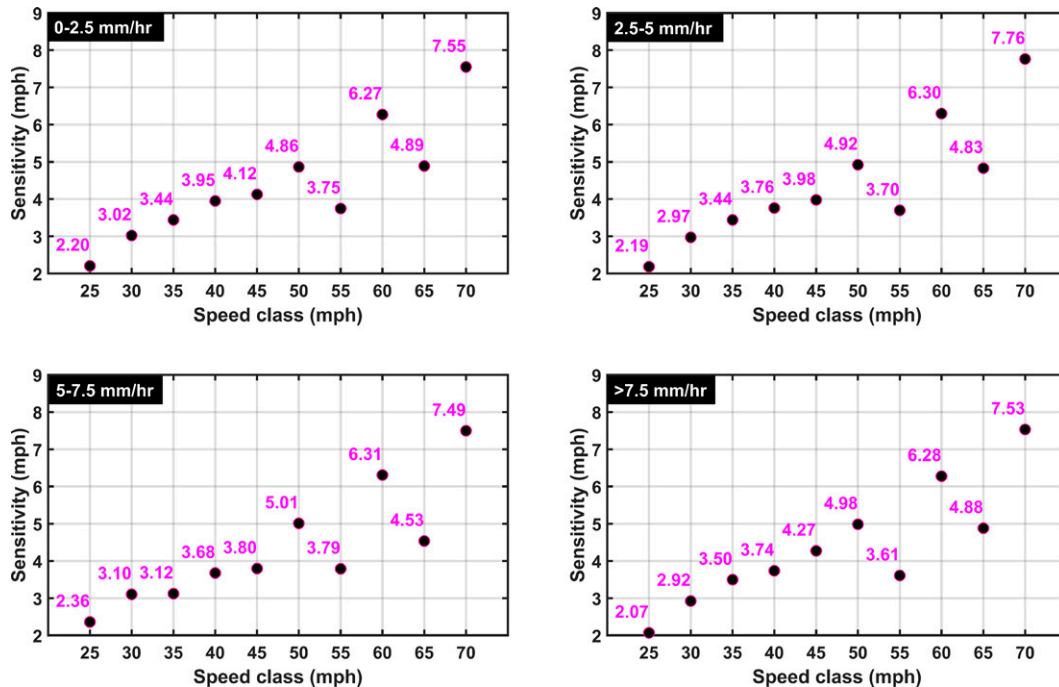


FIG. 2. Average sensitivity of traffic speed for rainfall intensities falling within the range (top left) $0\text{--}2.5\text{ mm h}^{-1}$, (top right) $2.5\text{--}5\text{ mm h}^{-1}$, (bottom left) $5\text{--}7.5\text{ mm h}^{-1}$, and (bottom right) $>7.5\text{ mm h}^{-1}$ on TMCs belonging to different speed classes (identified on the basis of free-flow speed). Average sensitivity shows an overall increase with speed class, with lowest sensitivity for 25 mph and highest for 70 mph, except for two speed classes (55 and 65 mph).

~76% of road sections in Alabama are missing. All of the TMCs selected for this analysis are categorized into one of the 10 classes based on their FFSS. The number of TMCs falling within each class is tabulated in Table S1 in the online supplemental material, and the number of rainfall events encountered by the selected 1151 TMCs, categorized using rainfall intensity and speed classes, is tabulated in Table S2 in the online supplemental material.

f. Variations in traffic volume

Traffic volume on road sections could be an important factor controlling the traffic speed response to rainfall events. Although data of real-time traffic volume for all of the TMCs do not exist, it is well known that traffic volume usually varies 1) diurnally, with higher volume during office hours and lower volume otherwise, and 2) within the week, with higher volumes usually observed during weekdays. Here we use the hourly data of traffic volume (<https://www.fhwa.dot.gov/policyinformation/tables/tmasdata/>) that are available over the continental United States from 2011 onward until 2020 to identify the hours in the state that generally experiences high traffic and also assess how the average traffic varies between weekdays and weekends. These traffic volume data are mainly collected at specific locations (known as “count station”) on the roadways. Most of the roadways that are selected to gather the traffic volume data are interstate, U.S., and state highways. These data are used to assess diurnal variability of traffic volume (see Fig. S2 and the associated

description in the online supplemental material). From the diurnal variations of traffic volume for Alabama (see Fig. S3 in the online supplemental material), the hours 0700–1800 LT are identified as the daytime period, and the rest are considered to be the nighttime period. The data (see Fig. S4 in the online supplemental material) also indicate that traffic volume is indeed higher during weekdays versus weekends.

g. Consistency of traffic speed sensitivity

Consistency or constancy of speed sensitivity refers to the persistence of relative speed sensitivity among different TMCs or TMC classes for a range of rainfall intensities. Here, the consistency is quantified using a rank correlation matrix (at 5% significance level) of traffic speed sensitivity of different TMCs for different rainfall intensities. High rank correlation is an indication that the relative sensitivity among the TMCs is the same across the rainfall intensities. This can be further illustrated as follows. Consider five TMCs, namely T_1 , T_2 , T_3 , T_4 , and T_5 , belonging to the same speed class (e.g., 70 mph). Let 6.2, 7.5, 5.6, 8.2, and 4 mph be their average sensitivities when they encounter a rainfall with intensity between 0 and 2.5 mm h^{-1} . In ascending order of the sensitivities, these TMCs can be ranked as T_5 , T_3 , T_1 , T_2 , and T_4 . Let us assume that for rainfall intensity between 2.5 and 5 mm h^{-1} the ranks again remain the same (T_5 , T_3 , T_1 , T_2 , and T_4). This identical ranking of different TMCs across a range of rainfall intensities, or a rank correlation of 1, indicates that the considered road network has high

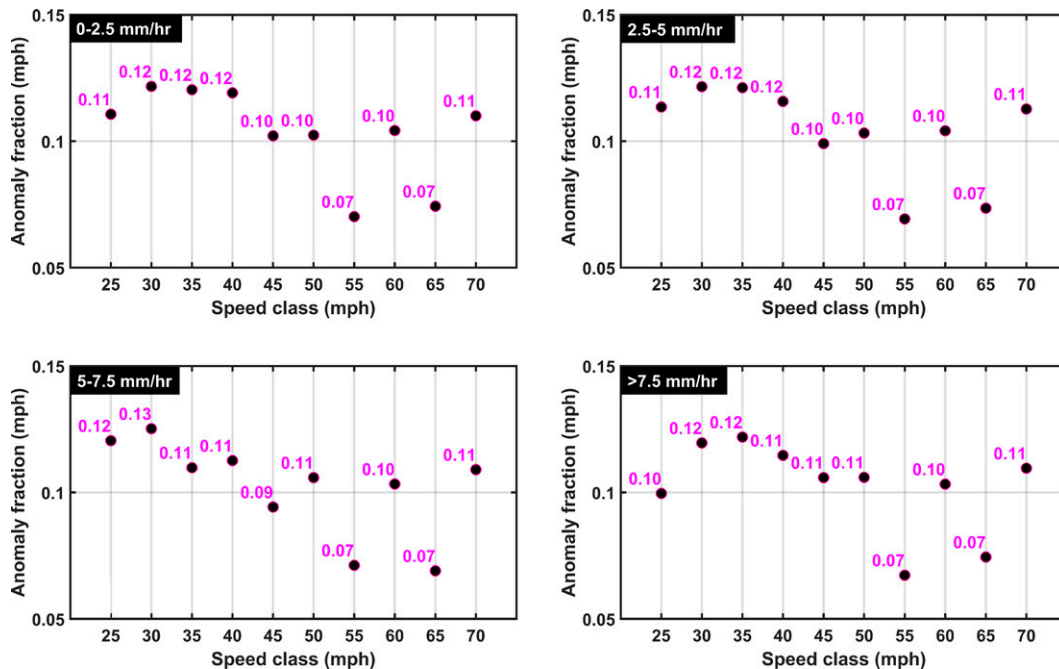


FIG. 3. Mean speed anomaly fraction categorized on the basis of speed classes and rainfall intensities: (top left) $0\text{--}2.5\text{ mm h}^{-1}$, (top right) $2.5\text{--}5\text{ mm h}^{-1}$, (bottom left) $5\text{--}7.5\text{ mm h}^{-1}$, and (bottom right) $>7.5\text{ mm h}^{-1}$. For most of the speed class and rainfall intensity combinations, speed anomaly fraction (sensitivity/reference speed) is between 0.09 and 0.12.

consistency in traffic speed sensitivity. Notably, if a road network has high consistency at two rainfall intensities, relative vehicle speed sensitivity observations made at a rainfall intensity that is more frequent can be used to develop a map of relative sensitivity. Here, consistencies are evaluated in three configurations:

- 1) consistency of all 1151 TMCs, irrespective of speed class, to assess whether TMCs retain their sensitivity ranks for rainfall events of different intensities,
- 2) consistency of TMCs grouped in speed classes to assess whether speed classes are a major descriptor of sensitivity ranks, and
- 3) consistency of TMCs within each speed class to assess the degree to which rank sensitivities within a speed class are retained for a range of rainfall intensities.

4. Results and discussion

a. Traffic speed sensitivity

Response of traffic speed to rainfall events is categorized based on the speed classes and rainfall intensities (see Fig. 2, along with Figs. S6 and S7 in the online supplemental material). Results show that the variations in average sensitivity across different speed classes are large in comparison with the variations across different rainfall intensities. Ancillary analysis indicates that the results (Fig. S8 in the online supplemental material) are robust to alternative definition of the dry pavement conditions (that considers current and

previous hours without rainfall) as outlined in section 3c. The results also highlight that the traffic speed sensitivity (reduction in speed) is relatively less influenced by variations in rainfall intensity. Sensitivity generally increases in magnitude from speed class 25 to 70 mph, although with some exceptions (e.g., for speed classes 55 and 65 mph). Notably, the magnitude of sensitivity is generally proportional to the reference speed of the speed class. This is evident in Fig. 3 where the average speed anomaly fraction or the average ratio of sensitivity to reference speed is plotted. Other than for the atypical sensitivity speed classes (55 and 65 mph), the speed anomaly fraction hovers within a narrow range of 0.09–0.12.

Further analysis is carried out to identify the possible reasons behind conspicuous sensitivity of two speed classes, 55 and 65 mph, with regard to the overall increasing trend with speed class. These speed classes will be termed as “atypical speed classes” for the ensuing discussion. First, a comparison is made between mean reference speed (Fig. S5 in the online supplemental material) of atypical speed classes with adjacent “normal” speed classes, 50 and 70 mph. During daytime period of week days, the mean reference speeds of atypical speed classes are close to the marked speeds of the corresponding speed class. However, for the normal classes, the average reference speeds during daytime period of weekdays are less than the marked speed. The daily averages of reference speeds for atypical and normal classes further confirm this observation (see Fig S5). For example, the daily average of reference speed for the atypical class 55 mph (in red) for

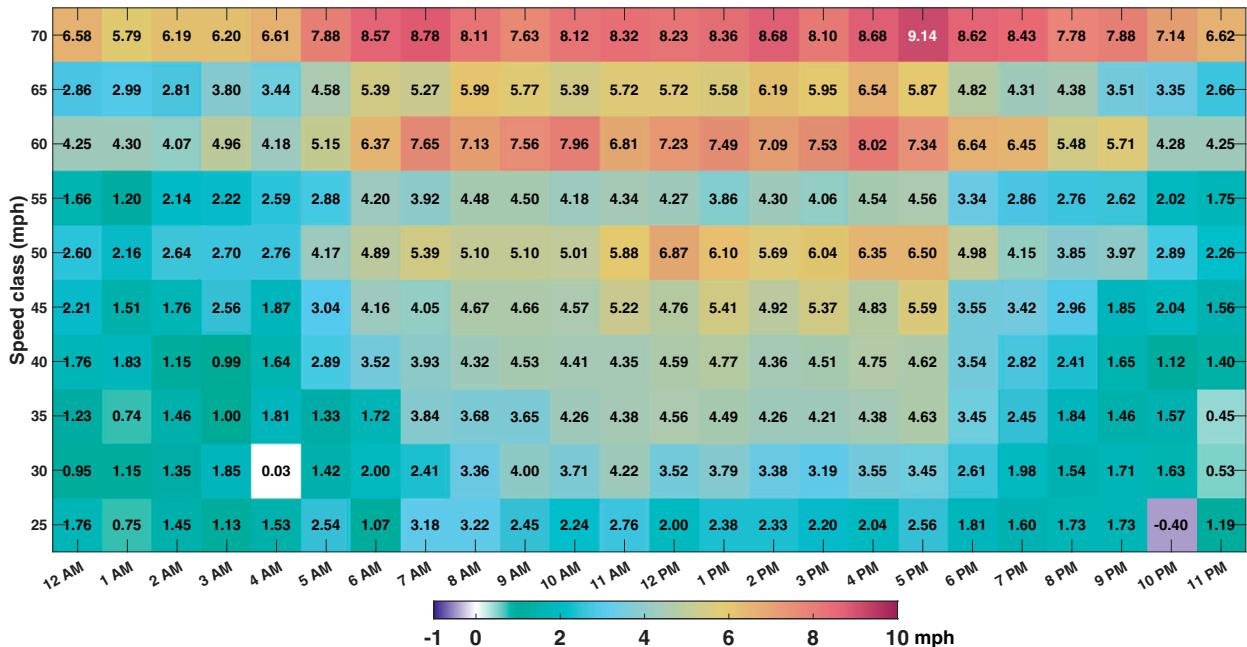


FIG. 4. Heat map depicting the role of diurnal variations in traffic volume on traffic speed sensitivity (mph) to rainfall. Influence of contrast in traffic during daytime period (0700–1800 LT) vs nighttime period is apparent at all speed classes. Traffic speed sensitivity to rainfall is relatively high during the daytime period for each speed class. The values noted on each grid of the heat map are the magnitudes of traffic speed sensitivity (mph) for the given time and speed class.

Monday is 55.168 mph, which is a bit higher than the marked speed of the class (55 mph). In contrast, for the normal class 50 mph (in blue), the reference speed average of 48.958 mph is lower than the marked speed of the class. Given that the reference speed is obtained for dry pavement conditions (see section 3b), a larger reference speed than marked speed in atypical speed classes indicate that these classes are overall less affected by ancillary conditions such as traffic volumes, traffic lights, and lane configurations. In contrast, a smaller reference speed with respect to the marked speed in the normal classes indicates appreciable effects of ancillary conditions. Because the impediments to free-flow speed are relatively less on the TMCs belonging to atypical speed classes, a smaller reduction in speed of the vehicle is needed during rainy conditions to ensure safe driving, thus also leading to lower traffic speed sensitivity.

Traffic speed sensitivity results presented above are based on consideration of four selected rainfall classes (see section 3e). To assess if the primary conclusions about the outsized influence of speed class with regard to the rainfall intensity on traffic speed sensitivity are valid for other rainfall intensity classifications, evaluations are also carried out with two additional sets of rainfall classes. The first set consists of rainfall classes such as 0–1, 1–2, 2–3, and >3 mm h⁻¹. The frequencies of rainfall events belonging to each class are provided in Table S3 in the online supplemental material. The second set involves dividing data belonging to each speed class into four equal parts (quartiles). The quartile rainfall intensities for each speed class are reported in Table S4 in the online supplemental material. This

selection criterion rules out the possibility of biases because of unequal sample size in each class that may affect the results. Average traffic speed sensitivity shows similar variations for the two (see Figs. S6 and S7 in the online supplemental material), and do not differ significantly from those obtained with the rainfall classes mentioned in section 3c. Hence, further analysis is carried out with the rainfall classes as discussed in section 3c. Although, it may be hypothesized that the sensitivity should be proportional to rainfall intensity, our results do not support this hypothesis. This could be due to the influence of traffic signals and signage, which may overwhelm the increasing influence of rainfall intensity. Notably, for the second set (supplemental Fig. S7), for which data belonging to each speed class are divided into four equal parts (equal sample size) and speed class is 70 mph, we do observe a small increasing trend.

b. Does traffic speed sensitivity of TMCs depend on traffic volume?

To assess whether traffic speed sensitivity depends on variations in traffic volume within a TMC, first the diurnal time series of sensitivity for each TMC speed class is obtained. Diurnal variations in the sensitivity for different speed classes (Fig. 4) reveal clear interaction between traffic volume and speed classes. For all speed classes, relatively high average sensitivity is observed during daytime period (0700–1800 LT). Overall, the magnitude of sensitivity is maximum for speed class 70 mph, and it seems to decrease with speed. In case of two atypical speed classes (55 and 65 mph), drop in the speed sensitivity is encountered, possibly due to low intervening

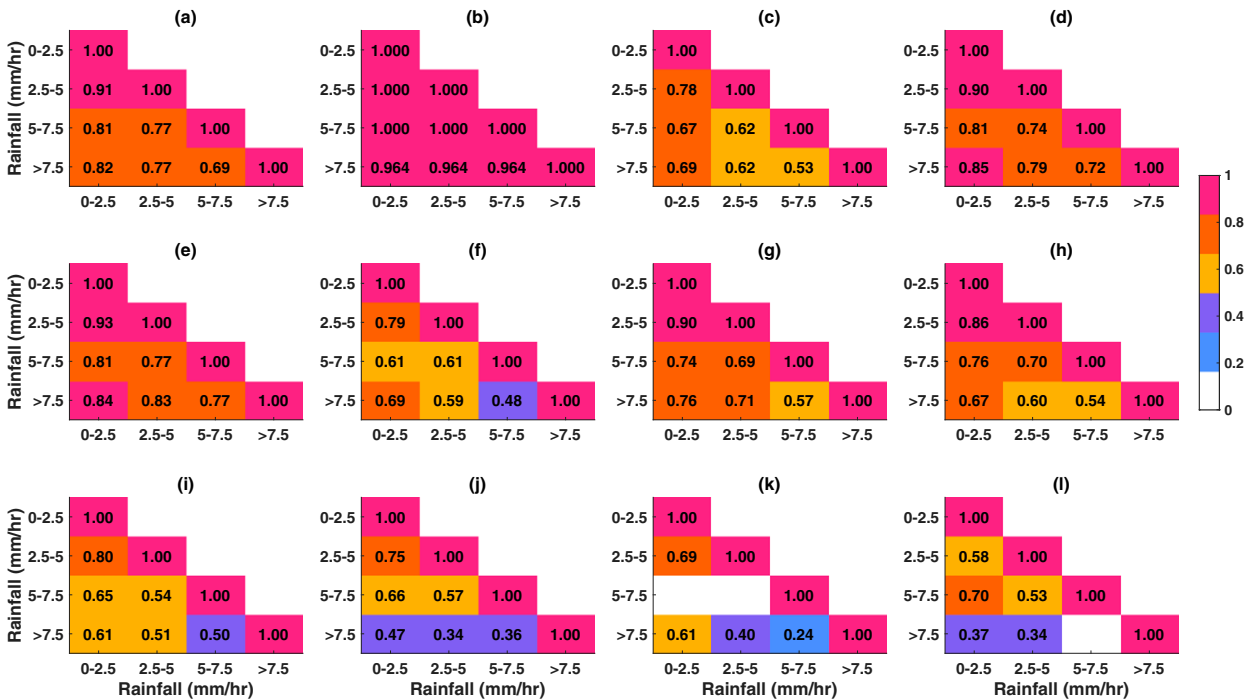


FIG. 5. Consistency analysis of traffic speed sensitivity. Consistency is quantified as rank correlation (at 5% significance level) of traffic speed sensitivity for different precipitation intensities (a) across all TMCs, (b) across TMC speed classes, and within TMC speed class (c) 70 mph, (d) 65 mph, (e) 60 mph, (f) 55 mph, (g) 50 mph, (h) 45 mph, (i) 40 mph, (j) 35 mph, (k) 30 mph, and (l) 25 mph. A high degree of consistency prevails across all TMCs and TMC speed classes, indicating that relative sensitivity is retained irrespective of the rainfall intensity. Within TMCs belonging to a speed class, except for low speed classes (35 mph and below), a moderate to high (≥ 0.5) consistency is observed.

variables to traffic (see section 4a). As discussed in section 3f, differences in traffic volume between weekdays and weekends are likely to affect the traffic sensitivity as well. To evaluate this, a similar analysis is carried out separately for weekdays (from Monday to Friday) and weekend. Average diurnal variations during weekdays (Fig. S9 in the online supplemental material) reveal a similar sensitivity pattern as that in case of average diurnal variations for all the days in a week (Fig. 4). However, average diurnal variation during weekend (Fig. S10 in the online supplemental material) is noisier. This is likely due to reduced diurnality of traffic volume on weekend, overall lesser traffic, and fewer data points for each rain intensity.

c. Consistency across rainfall intensities

Consistency is evaluated in three different ways (as discussed in section 3g) to gauge the relative traffic sensitivity of TMCs vis-à-vis rainfall intensity (see Fig. 5). A consistency matrix using the entire suite of 1151 TMCs (Fig. 5a) reveals a strong correlation (≥ 0.69) indicating relative sensitivity is retained irrespective of the rainfall intensity. A very high consistency (>0.95) is observed when obtained using average sensitivities for each speed class (Fig. 5b). This indicates overall relative rank of speed sensitivity between TMCs belonging to different speed classes can be explained to a high degree just based on the measurements conducted during one the rainfall intensity classes. To assess

the consistency within the speed classes, similar consistency matrices pertaining to different speed classes (Figs. 5c–l) are obtained. Based on these consistencies, it is observed that, for speed classes 70 to 40 mph, a moderate to high (≥ 0.5) correlation is observed, indicating high consistency. For low speed classes such as 30–25 mph, for some of the cases, the correlation is not statistically significant (shown by white background).

5. Summary and conclusions

Reduction in traffic flow speed is an expected response when rainfall events are encountered. However, the extent of reduction in speed and the role of ancillary controls on it are yet to be delineated. This study furnishes the aforementioned knowledge gaps by quantifying the sensitivity of traffic speed of road sections to rainfall events. Our result first confirms that rainfall indeed results in reduction in traffic speed. Results also indicate that the extent of reduction in traffic speed in response to rain events is dominantly influenced by the speed class category in which a road section falls (defined by TMC in this analysis) as compared with the rainfall intensity.

Even though, in terms of magnitude, it is observed that high-speed-class TMCs are more sensitive to rainfall, the speed reduction per unit free-flow speed of a road section generally falls within a narrow range of 0.09–0.12. We also find that

temporal variations of traffic volume both at subdaily and weekly scale influence the extent of speed reduction vis-à-vis rainfall intensity. Further analyses on the relative sensitivity of road sections to rainfall intensity reveals a fair amount of consistency across rainfall intensities. The consistency across TMCs belonging to different speed classes is very high, with rank correlation of sensitivity being often larger than 0.95. In other words, relative sensitivity between TMCs belonging to different speed classes for extreme precipitation events (e.g., hourly intensity $>7.5 \text{ mm h}^{-1}$) can be evaluated with confidence just by obtaining vehicle speed data during low but frequent precipitation events (e.g., hourly intensity $<2.5 \text{ mm h}^{-1}$). A rank correlation of ≥ 0.69 is observed when considering all TMCs, which highlights that the relative sensitivity between different TMCs is largely retained irrespective of the rainfall intensity. Overall, the study demonstrates a novel use of crowdsourced probe vehicle data to understand the sensitivity of road sections to precipitation and also maps the relative sensitivity of different road sections to precipitation events. The latter information can be used to prioritize weather-aware road design, traffic management, and signage in regions with high traffic speed sensitivity.

The sensitivity analysis carried out here can also be used as a starting point for future related explorations. For example, the role of traffic signals, lane configurations, and other traffic influencing factors on traffic speed sensitivity has not been evaluated here. For settings with real-time traffic data, the analyses can be extended to study how the sensitivity is driven by traffic volume and other dynamic characteristics.

Acknowledgments. Funding was provided by an Alabama Transportation Institute seed grant (to author Kumar). Author contributions were as follows—conceptualization: Kumar; method: Kumar and authors Salvi and Hainen; software: Salvi; validation: Salvi; formal analysis: Kumar and Salvi; investigation: Kumar, Hainen, and Salvi; data acquisition: Hainen; writing—original draft: Salvi; writing—review and editing: Kumar and Hainen; visualization: Kumar and Salvi; supervision: Kumar and Hainen; project administration: Kumar; funding acquisition: Kumar. The authors declare that they have no competing interests.

Data availability statement. The data used in this paper can be downloaded from the following websites: NLDAS precipitation and temperature hourly data: <https://disc.gsfc.nasa.gov/datasets?keywords=NLDAS>. Crowdsourced speed data: Raw data are restricted for share by the data custodian. Processed data are, however, provided at <https://doi.org/10.5281/zenodo.6617331>. Traffic volume data (hourly): <https://www.fhwa.dot.gov/policyinformation/tables/tmasdata/>. The data derived using original crowdsourced data for 1151 TMCs, their reference matrices, and sensitivities are available from the following link, along with the codes to generate these files: <https://doi.org/10.5281/zenodo.6617331>. The following software was used for the analysis and figure generation: ARCGIS ArcMAP 10.6.1, R-Studio Version 1.2.5001, and MATLAB R2021a.

REFERENCES

- Abdulla, B., A. Kiaghadi, H. S. Rifai, and B. Birgisson, 2020: Characterization of vulnerability of road networks to fluvial flooding using SIS network diffusion model. *J. Infrastruct. Preserv. Resilience*, **1**, 6, <https://doi.org/10.1186/s43065-020-00004-z>.
- Al-Hamdan, M. Z., and Coauthors, 2014: Environmental public health applications using remotely sensed data. *Geocarto Int.*, **29**, 85–98, <https://doi.org/10.1080/10106049.2012.715209>.
- Alizadeh-Choobari, O., and M. S. Najafi, 2018: Extreme weather events in Iran under a changing climate. *Climate Dyn.*, **50**, 249–260, <https://doi.org/10.1007/s00382-017-3602-4>.
- Andrey, J., B. Mills, M. Leahy, and J. Suggett, 2003: Weather as a chronic hazard for road transportation in Canadian cities. *Nat. Hazards*, **28**, 319–343, <https://doi.org/10.1023/A:1022934225431>.
- Auer, A. H., Jr., 1974: The rain versus snow threshold temperatures. *Weatherwise*, **27**, 67, <https://doi.org/10.1080/00431672.1974.9931684>.
- Bae, B., H. Kim, H. Lim, Y. Liu, L. D. Han, and P. B. Freeze, 2018: Missing data imputation for traffic flow speed using spatio-temporal cokriging. *Transp. Res.*, **88**, 124–139, <https://doi.org/10.1016/j.trc.2018.01.015>.
- Barjenbruch, K., and Coauthors, 2016: Drivers' awareness of and response to two significant winter storms impacting a metropolitan area in the intermountain west: Implications for improving traffic flow in inclement weather. *Wea. Climate Soc.*, **8**, 475–491, <https://doi.org/10.1175/WCAS-D-16-0017.1>.
- Barrett, B., B. Ran, and R. Pillai, 2000: Developing a dynamic traffic management modeling framework for hurricane evacuation. *Transp. Res. Rec.*, **1733**, 115–121, <https://doi.org/10.3141/1733-15>.
- Bartlett, A., W. Lao, Y. Zhao, and A.W. Sadek, 2013: Impact of inclement weather on hourly traffic volumes in Buffalo, New York. *Transportation Research Board 92nd Annual Meeting*, Washington, DC, Transportation Research Board, 13-3240, <https://trid.trb.org/view/1241923>.
- Beven, K., 1993: Prophecy, reality and uncertainty in distributed hydrological modelling. *Adv. Water Resour.*, **16**, 41–51, [https://doi.org/10.1016/0309-1708\(93\)90028-E](https://doi.org/10.1016/0309-1708(93)90028-E).
- Billot, R., N.-E. El Faouzi, and F. De Vuyst, 2009: Multilevel assessment of the impact of rain on drivers' behavior: Standardized methodology and empirical analysis. *Transp. Res. Rec.*, **2107**, 134–142, <https://doi.org/10.3141/2107-14>.
- Black, A. W., G. Villarini, and T. L. Mote, 2017: Effects of rainfall on vehicle crashes in six US states. *Wea. Climate Soc.*, **9**, 53–70, <https://doi.org/10.1175/WCAS-D-16-0035.1>.
- Calvert, S. C., and M. Snelder, 2018: A methodology for road traffic resilience analysis and review of related concepts. *Transportmetrica*, **14A**, 130–154, <https://doi.org/10.1080/23249935.2017.1363315>.
- Chen, X., M. Kumar, D. deB. Richter, and Y. Mau, 2020: Impact of gully incision on hillslope hydrology. *Hydrol. Processes*, **34**, 3848–3866, <https://doi.org/10.1002/hyp.13845>.
- Cope, J. T., B. F. Alvord, and A. E. Drake, 1962: Rainfall distribution in Alabama. *Agricultural Experiment Station Progress Rep.* 84, 6 pp., <https://aurora.auburn.edu/bitstream/handle/11200/1386/0523PROG.pdf?sequence=1&isAllowed=y>.
- Cosgrove, B. A., and Coauthors, 2003: Real-time and retrospective forcing in the North American Land Data Assimilation System (NLDAS) project. *J. Geophys. Res.*, **108**, 8842, <https://doi.org/10.1029/2002JD003118>.

- Dai, A., 2008: Temperature and pressure dependence of the rain-snow phase transition over land and ocean. *Geophys. Res. Lett.*, **35**, L12802, <https://doi.org/10.1029/2008GL033295>.
- Gainin, A. A., M. Kitsak, D. Marchese, J. M. Keisler, T. Seager, and I. Linkov, 2017: Resilience and efficiency in transportation networks. *Sci. Adv.*, **3**, e1701079, <https://doi.org/10.1126/sciadv.1701079>.
- Gauthier, P., A. Furno, and N. E. El Faouzi, 2018: Road network resilience: How to identify critical links subject to day-to-day disruptions. *Transp. Res. Rec.*, **2672**, 54–65, <https://doi.org/10.1177/0361198118792115>.
- Han, F., and S. Zhang, 2020: Evaluation of spatial resilience of highway networks in response to adverse weather conditions. *ISPRS Int. J. Geoinf.*, **9**, 480, <https://doi.org/10.3390/ijgi9080480>.
- Hosseiniou, M. H., S. A. Kheyabadi, and A. Zolfaghari, 2015: Determining optimal speed limits in traffic networks. *IATSS Res.*, **39**, 36–41, <https://doi.org/10.1016/j.iatssr.2014.08.003>.
- Hranac, R., E. Sterzin, D. Krechmer, H. Rakha, and M. Farzaneh, 2006: Empirical studies on traffic flow in inclement weather. U.S. Department of Transportation Tech. Rep. FHWA-HOP-07-073, 108 pp., <https://rosap.ntl.bts.gov/view/dot/42251>.
- IPCC, 2021: *Climate Change 2021: The Physical Science Basis*. V. Masson-Delmotte et al., Eds., Cambridge University Press, 2391 pp., https://www.ipcc.ch/report/ar6/wg1/downloads/report/IPCC_AR6_WGI_FullReport.pdf.
- Islam, N., E. K. Adanu, A. M. Hainen, S. Burdette, R. Smith, and S. Jones, 2021: A comparative analysis of freeway crash incident clearance time using random parameter and latent class hazard-based duration model. *Accid. Anal. Prev.*, **160**, 106303, <https://doi.org/10.1016/j.aap.2021.106303>.
- Israel, G. D., 1992: Determining sample size. University of Florida IFAS Extension Fact Sheet PEOD-6, 5 pp., https://www.gjimt.ac.in/wp-content/uploads/2017/10/2_Glenn-D.-Israel_Determining-Sample-Size.pdf.
- Jenelius, E., T. Petersen, and L. G. Mattsson, 2006: Importance and exposure in road network vulnerability analysis. *Transp. Res.*, **40**, 537–560, <https://doi.org/10.1016/j.tra.2005.11.003>.
- Jennings, K. S., T. S. Winchell, B. Livneh, and N. P. Molotch, 2018: Spatial variation of the rain-snow temperature threshold across the Northern Hemisphere. *Nat. Commun.*, **9**, 1148, <https://doi.org/10.1038/s41467-018-03629-7>.
- Lam, W. H., M. L. Tam, X. Cao, and X. Li, 2013: Modeling the effects of rainfall intensity on traffic speed, flow, and density relationships for urban roads. *J. Transp. Eng.*, **139**, 758–770, [https://doi.org/10.1061/\(ASCE\)TE.1943-5436.0000544](https://doi.org/10.1061/(ASCE)TE.1943-5436.0000544).
- Lewis, C. S., H. M. Geli, and C. M. Neale, 2014: Comparison of the NLDAS weather forcing model to agrometeorological measurements in the western United States. *J. Hydrol.*, **510**, 385–392, <https://doi.org/10.1016/j.jhydrol.2013.12.040>.
- Lu, H., 2014: Short-term traffic prediction using rainfall. *Int. J. Signal Process. Syst.*, **2**, 70–73, <http://doi.org/10.12720/ijsp.2.1.70-73>.
- Ludlow, F., and C. Travis, 2019: STEAM approaches to climate change, extreme weather and social-political conflict. *The STEAM Revolution*, A. de la Garza and C. Travis, Eds., Springer, 33–65.
- Marks, D., A. Winstral, M. Reba, J. Pomeroy, and M. Kumar, 2013: An evaluation of methods for determining during-storm precipitation phase and the rain/snow transition elevation at the surface in a mountain basin. *Adv. Water Resour.*, **55**, 98–110, <https://doi.org/10.1016/j.advwatres.2012.11.012>.
- Martín, B., E. Ortega, R. Cuevas-Wizner, A. Ledda, and A. De Montis, 2021: Assessing road network resilience: An accessibility comparative analysis. *Transp. Res.*, **95**, 102851, <https://doi.org/10.1016/j.trd.2021.102851>.
- Mathew, S., and S. S. Pulugurtha, 2022: Quantifying the effect of rainfall and visibility conditions on road traffic travel time reliability. *Wea. Climate Soc.*, **14**, 507–519, <https://doi.org/10.1175/WCAS-D-21-0053.1>.
- Nogal, M., A. O'Connor, B. Martinez-Pastor, and B. Caulfield, 2017: Novel probabilistic resilience assessment framework of transportation networks against extreme weather events. *ASCE-ASME J. Risk Uncertainty Eng. Syst.*, **3A**, 04017004, <https://doi.org/10.1061/AJRUA6.0000908>.
- Omrnian, E., H. Sharif, S. Dessouky, and J. Weissmann, 2018: Exploring rainfall impacts on the crash risk on Texas roadways: A crash-based matched-pairs analysis approach. *Accid. Anal. Prev.*, **117**, 10–20, <https://doi.org/10.1016/j.aap.2018.03.030>.
- Ortega, E., B. Martín, and Á. Aparicio, 2020: Identification of critical sections of the Spanish transport system due to climate scenarios. *J. Transp. Geogr.*, **84**, 102691, <https://doi.org/10.1016/j.jtrangeo.2020.102691>.
- Pan, M., and Coauthors, 2003: Snow process modeling in the North American Land Data Assimilation System (NLDAS): 2. Evaluation of model simulated snow water equivalent. *J. Geophys. Res.*, **108**, 8850, <https://doi.org/10.1029/2003JD003994>.
- Pregolato, M., A. Ford, S. M. Wilkinson, and R. J. Dawson, 2017: The impact of flooding on road transport: A depth-disruption function. *Transp. Res.*, **55**, 67–81, <https://doi.org/10.1016/j.trd.2017.06.020>.
- Prokhorchuk, A., N. Mitrovic, U. Muhammad, A. Stevanovic, M. T. Asif, J. Dauwels, and P. Jaillot, 2021: Estimating the impact of high-fidelity rainfall data on traffic conditions and traffic prediction. *Transp. Res. Rec.*, **2675**, 1285–1300, <https://doi.org/10.1177/03611981211026309>.
- Rakha, H., M. Farzaneh, M. Arafeh, and E. Sterzin, 2008: Inclement weather impacts on freeway traffic stream behavior. *Transp. Res. Rec.*, **2071**, 8–18, <https://doi.org/10.3141/2071-02>.
- Sarlas, G., A. Páez, and K. W. Axhausen, 2020: Betweenness-accessibility: Estimating impacts of accessibility on networks. *J. Transp. Geogr.*, **84**, 102680, <https://doi.org/10.1016/j.jtrangeo.2020.102680>.
- Schaake, J. C., and Coauthors, 2004: An intercomparison of soil moisture fields in the North American Land Data Assimilation System (NLDAS). *J. Geophys. Res.*, **109**, D01S90, <https://doi.org/10.1029/2002JD003309>.
- Sen, S., P. Srivastava, J. H. Dane, K. H. Yoo, and J. N. Shaw, 2010: Spatial-temporal variability and hydrologic connectivity of runoff generation areas in a North Alabama pasture—Implications for phosphorus transport. *Hydrol. Processes*, **24**, 342–356, <https://doi.org/10.1002/hyp.7502>.
- Sitterson, J., S. Sinnathamby, R. Parmar, J. Koblich, K. Wolfe, and C. D. Knightes, 2020: Demonstration of an online web services tool incorporating automatic retrieval and comparison of precipitation data. *Environ. Modell. Software*, **123**, 104570, <https://doi.org/10.1016/j.envsoft.2019.104570>.
- Souleyrette, R., T. H. Maze, and M. Agarwal, 2006: The weather and its impact on urban freeway traffic operations. *Proc. Transportation Research Board 85th Annual Meeting*, Washington, DC, Transportation Research Board, 06-1439, <https://trid.trb.org/view/776891>.
- Valenzuela, Y. B., R. S. Rosas, M. Mazari, M. Risse, and T. Rodriguez-Nikl, 2017: Resilience of road infrastructure in response to extreme weather events. *Int. Conf. on Sustainable Infrastructure*, New York, NY, ASCE, 349–360.

- Verendel, V., and S. Yeh, 2019: Measuring traffic in cities through a large-scale online platform. *J. Big Data Anal. Transp.*, **1**, 161–173, <https://doi.org/10.1007/s42421-019-00007-7>.
- Xia, Y., and Coauthors, 2012: Continental-scale water and energy flux analysis and validation for North American Land Data Assimilation System project phase 2 (NLDAS-2): 2. Validation of model-simulated streamflow. *J. Geophys. Res.*, **117**, D03110, <https://doi.org/10.1029/2011JD016051>.
- Xu, Y., L. Wang, K. W. Ross, C. Liu, and K. Berry, 2018: Standardized soil moisture index for drought monitoring based on soil moisture active passive observations and 36 years of North American land data assimilation system data: A case study in the southeast United States. *Remote Sens.*, **10**, 301, <https://doi.org/10.3390/rs10020301>.
- Zhang, B., Y. Xia, B. Long, M. Hobbins, X. Zhao, C. Hain, Y. Li, and M. C. Anderson, 2020: Evaluation and comparison of multiple evapotranspiration data models over the contiguous United States: Implications for the next phase of NLDAS (NLDAS-Testbed) development. *Agric. For. Meteorol.*, **280**, 107810, <https://doi.org/10.1016/j.agrformet.2019.107810>.

Supplementary information

Sensitivity of Traffic Speed to Rainfall

Kaustubh Anil Salvi¹, Mukesh Kumar^{2*}, Alexander M. Hainen²

¹Alabama Transportation Institute, University of Alabama; Tuscaloosa, AL 35487, USA.

²Department of Civil Construction & Environmental Engineering, University of Alabama, P.O. Box 870205,
Tuscaloosa, Alabama, 35487-0205

Corresponding Author: *Mukesh Kumar.

Address: Cyber hall, 248 Kirkbride Ln, Tuscaloosa, AL 35401

Email: mkumar4@eng.ua.edu; Phone: +1-205-348-0180

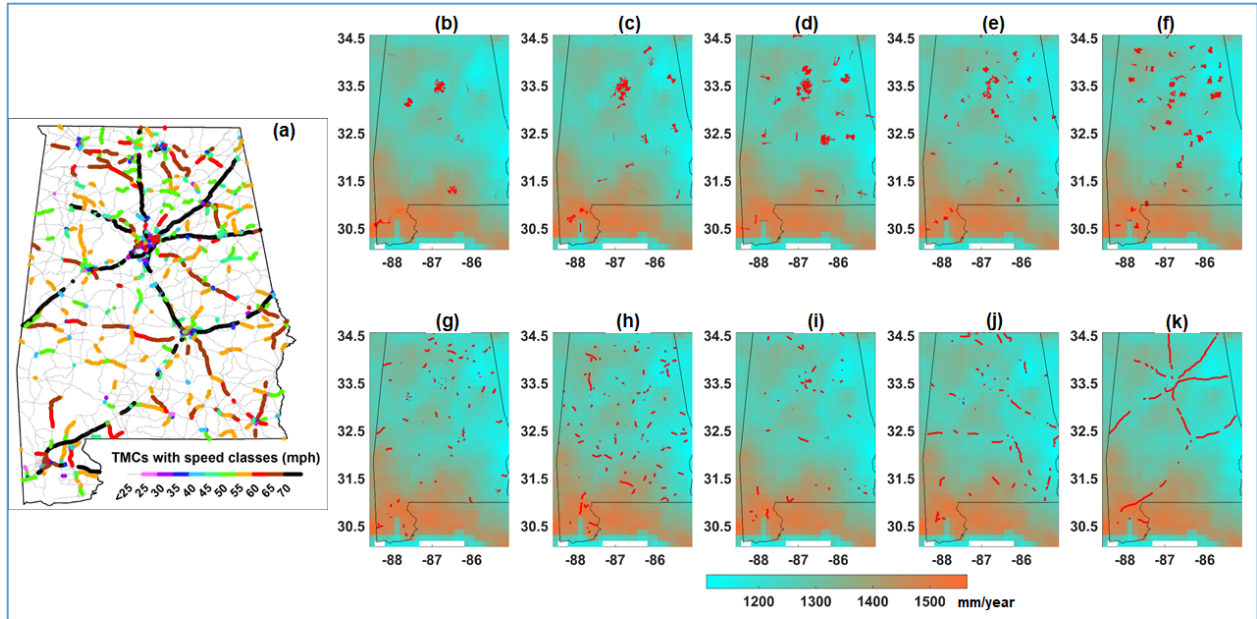


FIG S1: Geographic distribution of 1,151 TMCs (panel a) selected for the sensitivity analysis. Colors represent the speed classes derived based on the free-flow speed. Panel figures b to k highlight the geographic distribution of TMCs (in red) belonging to different speed classes (25 mph (b), 30 mph (c), 35 mph (d), 40 mph (e), 45 mph (f), 50 mph (g), 55 mph (h), 60 mph (i), 65 mph (j), 70 mph (k)). Background color in these panel figure show the annual average rainfall (mm) pattern over Alabama. Selected TMCs in each speed class encompass a range of precipitation regimes.

1. Traffic volume factors

Hourly data of traffic volumes at continental scale are available from 2011 to 2020 only for selected road sections (e.g., interstate, US, and state highways). Following is the stepwise procedure to obtain diurnal variations in traffic volume factors. Traffic volume factor is the ratio of traffic volume in a given hour and total traffic volume within a year.

- a) An hourly traffic volume factor time series for a given year is obtained using equation S1.

$$\text{Hourly Traffic Volume factor}_i = \frac{TV_i}{\sum_{i=1}^{NH} TV_i} \quad \dots (S1)$$

NH is the number of hours in the year and TV_i is the traffic volume in ‘ i^{th} ’ hour in the same year. Hence, hourly traffic volume factor (HTVF) for ‘ i^{th} ’ hour represents the fraction of the total hourly traffic volume in one year.

- b) Ten time series of HTVF (one of each year) are obtained and an average time series is calculated for Alabama. (dimension of average time series: 8784×1)
- c) The averaged time series is converted to 24 hour time series by obtaining mean HTVF for each hour. For example, mean HTVF for 1st hour of the day (12 AM) is obtained by calculating average HTVF of 366 values corresponding to 1st hour of the day (see figure S2). This time series is termed as diurnal traffic volume factor time series.

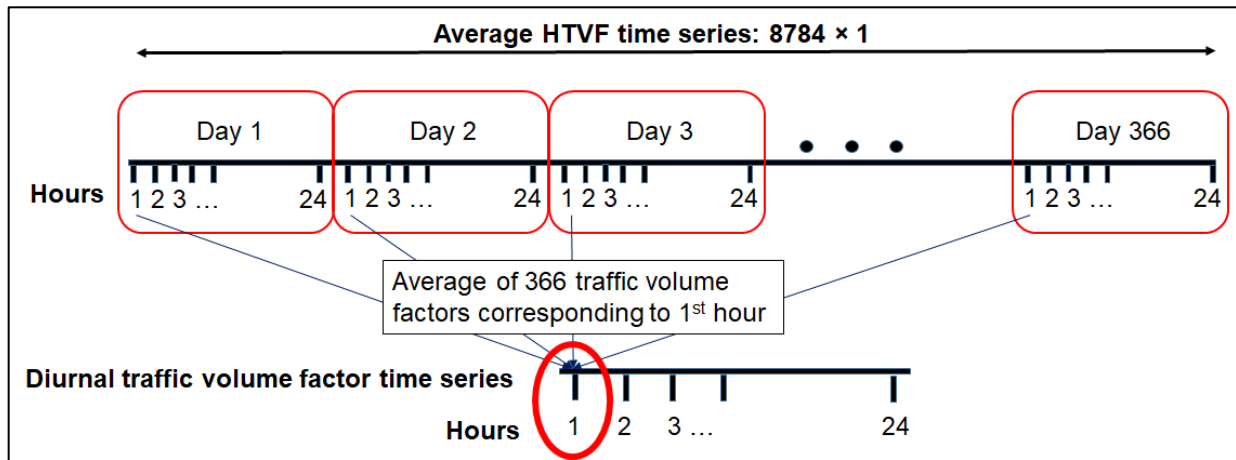


FIG S2: Pictorial representation of approach used to obtain diurnal traffic volume factor time series from average HTVF time series.

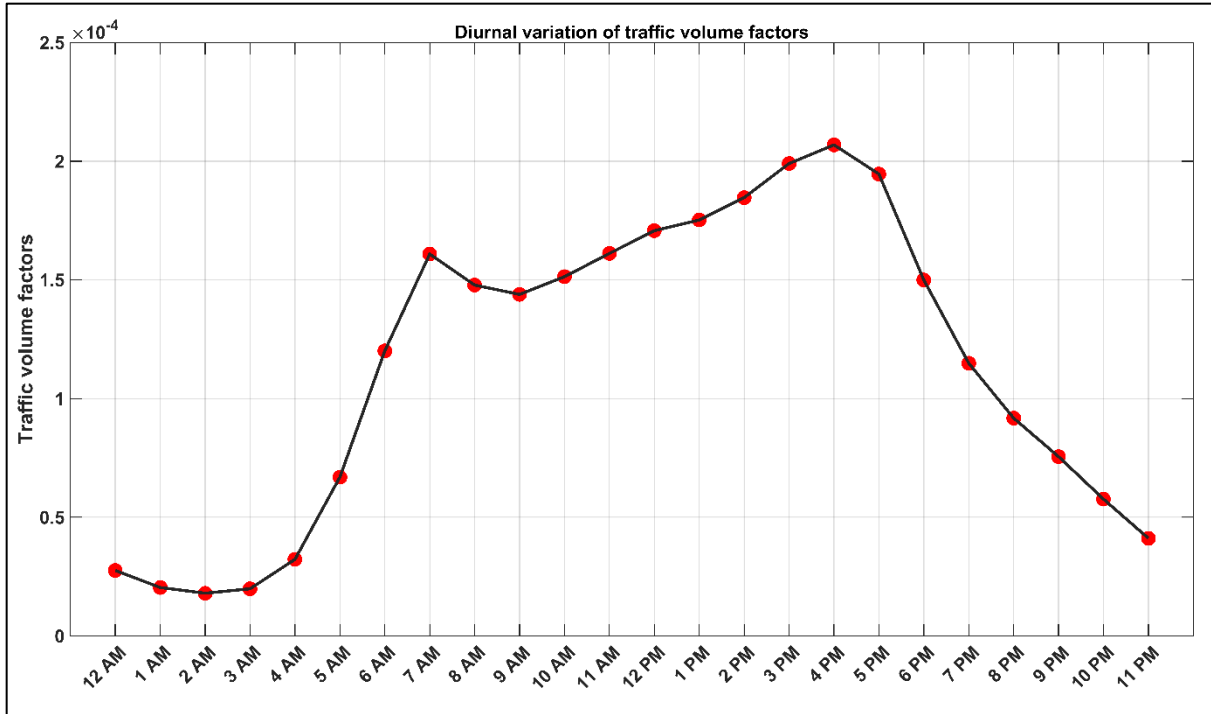


FIG S3: Diurnal traffic volume factor (see details in Supplementary text with figure S2) time series for Alabama. The plot shows the multiyear (2011-2020) average of diurnal variation of hourly fraction of total annual traffic volume. Based on the relatively high magnitude of factors during 7AM and 6PM, these hours can be identified as the daytime period. Before and after the daytime period, the series shows steep gradients before plummeting to low traffic volume factors during nighttime period.

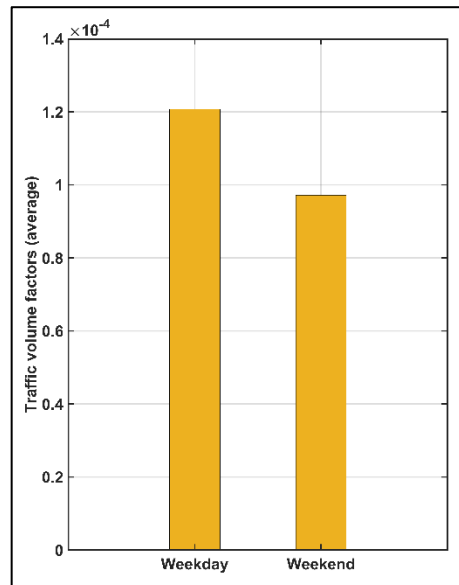


FIG S4: Average traffic volume factors during weekday and weekend. The traffic volume during weekday is higher in magnitude as compared to that during weekend.

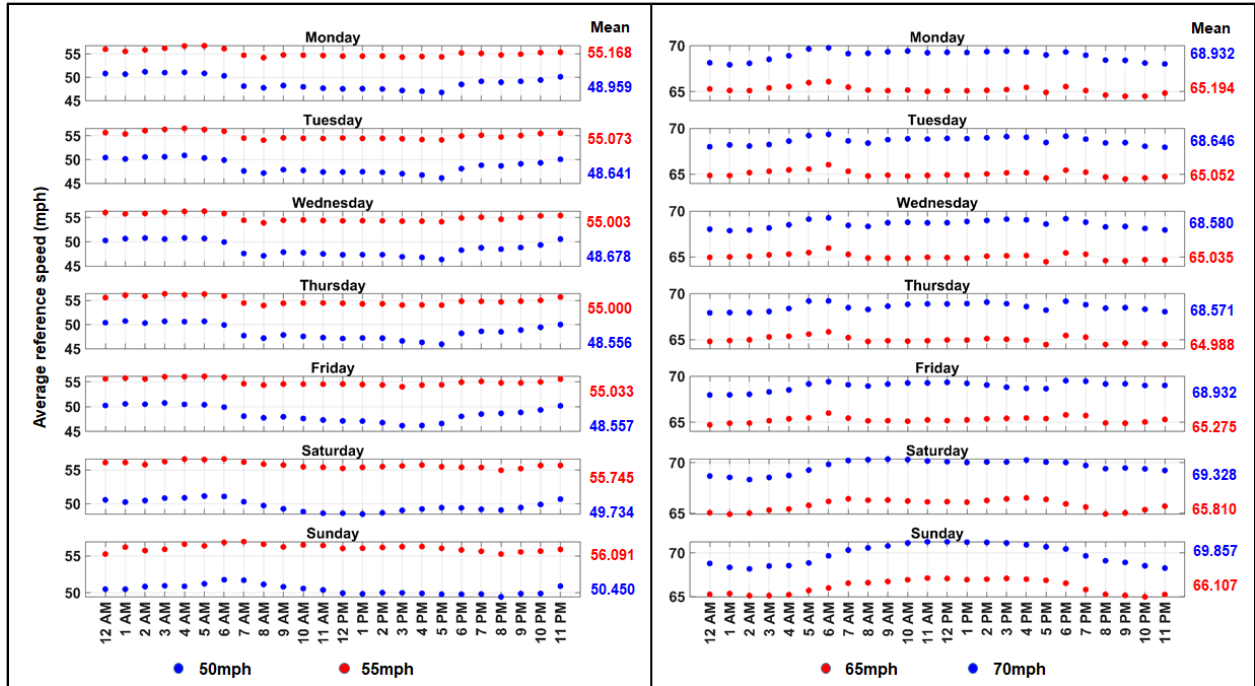


FIG S5: Day-wise diurnal variations in average reference speed of all TMCs belonging to atypical (i.e., speed class 55 and 65 mph shown by red dots) and normal (i.e., speed class 50 and 70 mph shown by blue dots) speed classes. Comparison of daily mean of reference speeds (in red for atypical classes and in blue for normal classes) indicate that reference speed for atypical (normal) classes are greater (smaller) than marked speeds.

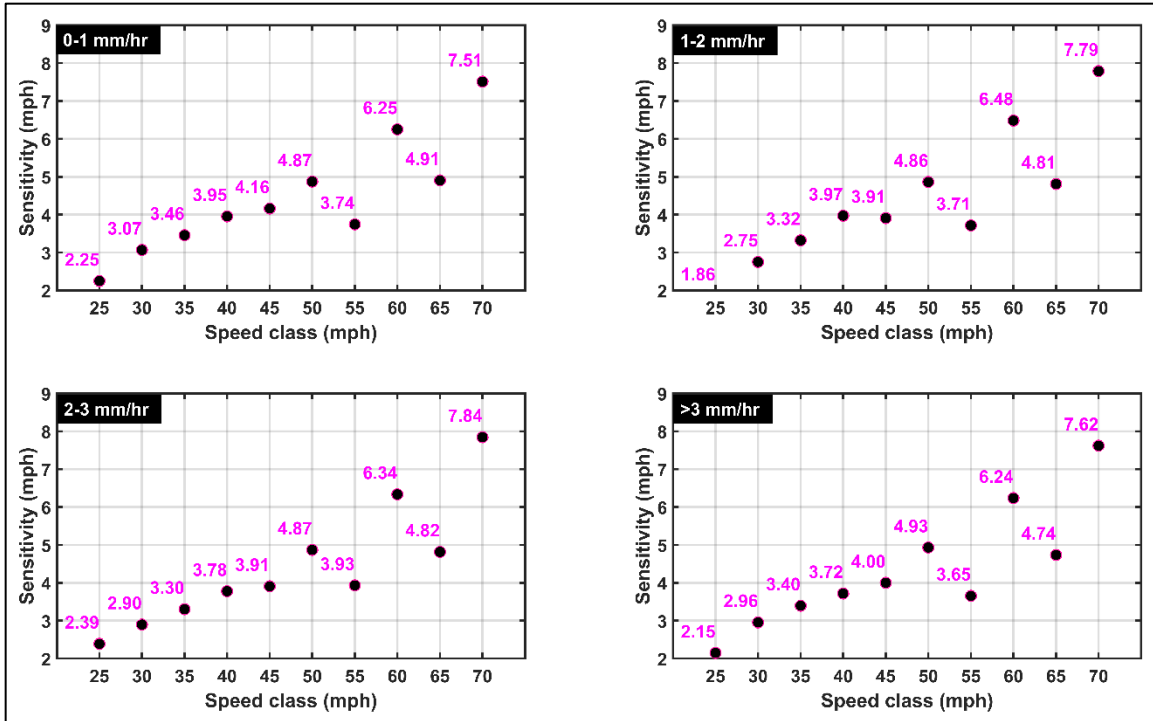


FIG S6: Similar to figure 2, but for rainfall classes 0-1 mm/hr, 1-2 mm/hr, 2-3 mm/hr, and >3 mm/hr

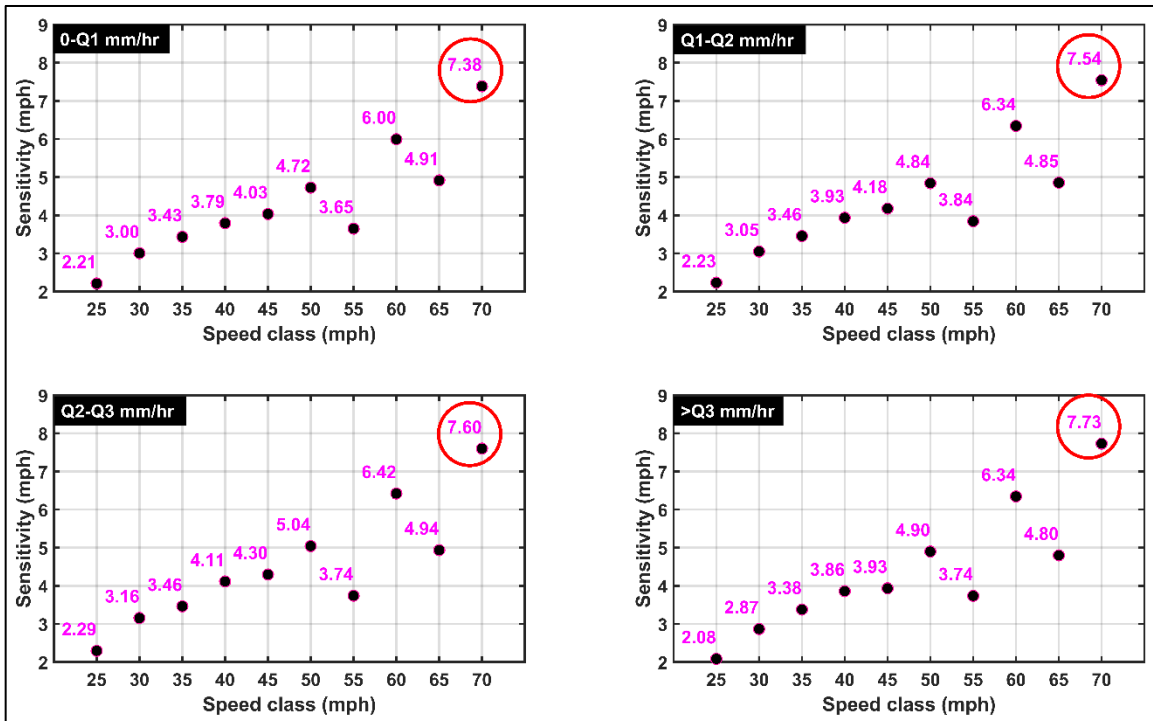


FIG S7: Similar to figure 2, but here each speed class is divided into four equal-sized parts (i.e. with identical sample sizes) in order of rainfall magnitude. Q1, Q2, and Q3 are first, second, and the third rainfall quartiles. Sensitivities for speed class 70 mph corresponding to different rainfall intensities (highlighted by red circle) which mostly consists of freeways without traffic signals show statistically significant increase ($pval < 0.05$) as compared to the sensitivity for 0-Q1 mm/hr implying effect of increase in rainfall intensity.

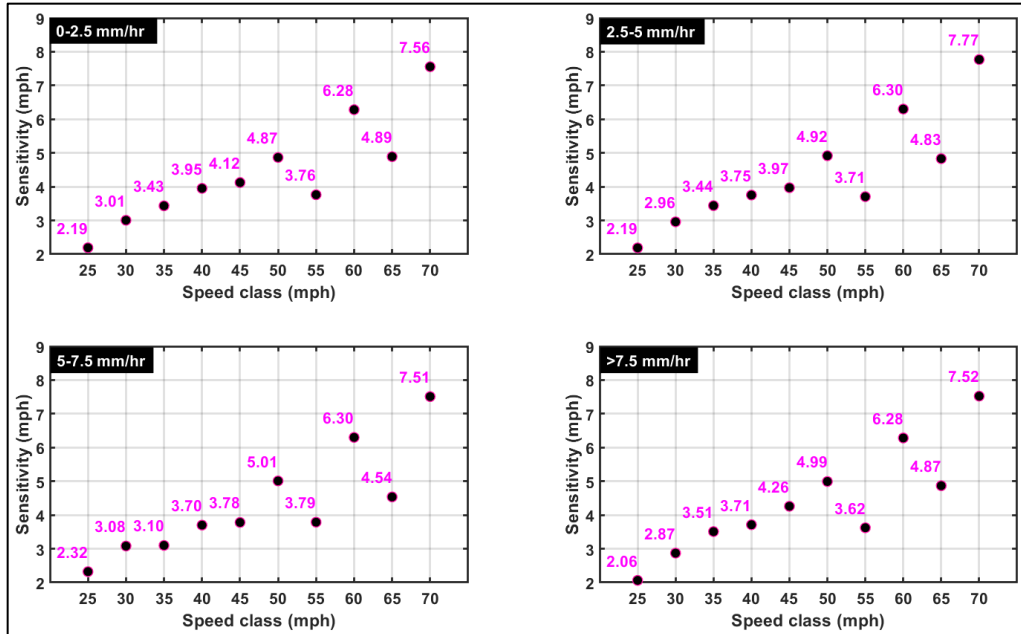


FIG S8: Same as FIG 2, but here for the reference speed calculation, a dry pavement is assumed to be prevalent when rainfall is equal to zero and temperature is greater than 4°C, both in the current and the last hour. In contrast, in FIG 2, dry pavement assumed zero precipitation only in the current hour.

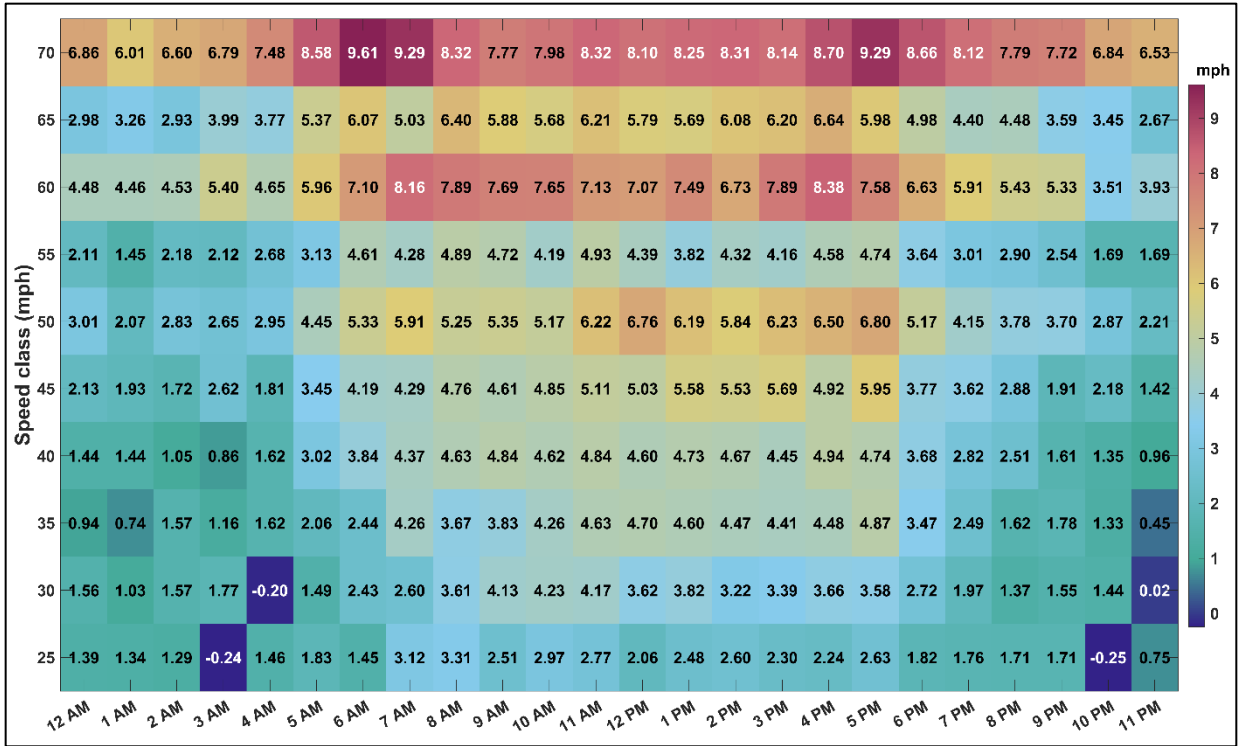


FIG S9: Role of traffic volume on diurnal variations in traffic speed sensitivity (mph) shown by heatmap during weekdays. Influence of variations in traffic during daytime period (7AM-6PM) and nighttime period is apparent at all speed classes. Traffic speed sensitivity to rainfall is relatively high during daytime period for each speed class. For better legibility, magnitudes of traffic speed sensitivity (pertaining to darker shades) are shown with white text.

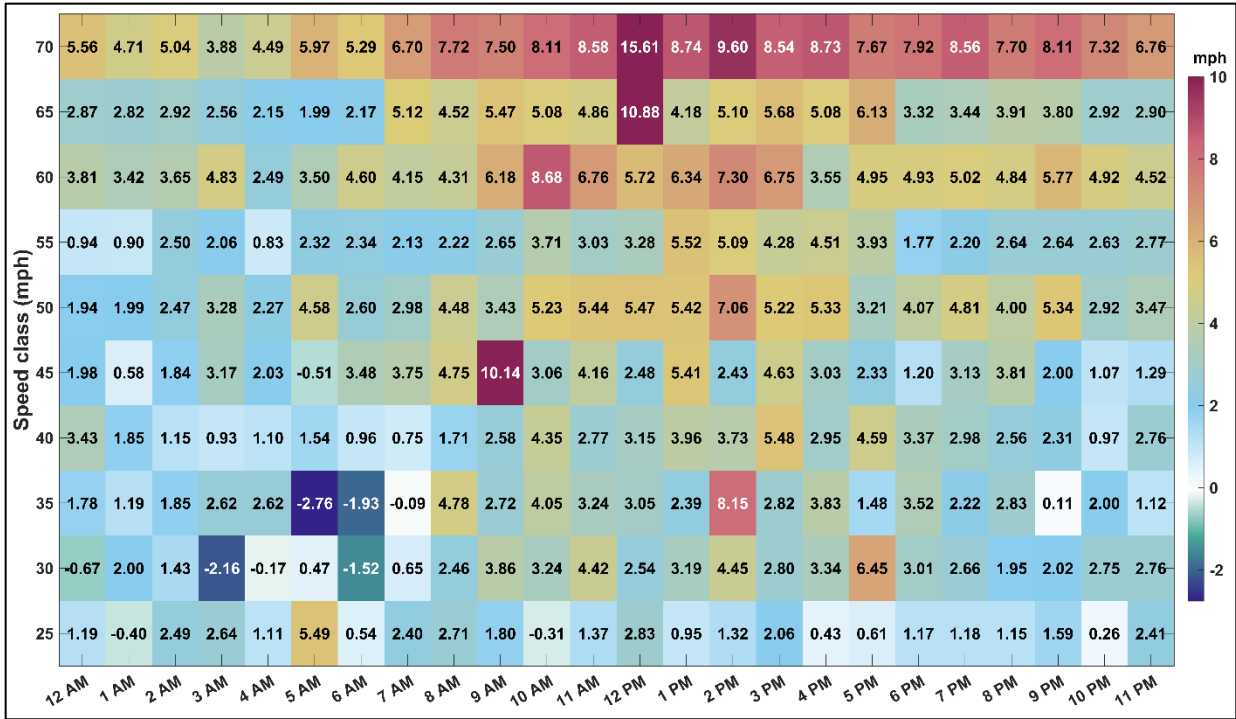


FIG S10: Similar to figure S9, however, this only shows diurnal variations of speed sensitivity during the weekend

Table S1: Frequency of road sections within each speed class.

No.	Speed class (mph)	Count
1	25 (FFS range 22.5-27.5)	49
2	30 (FFS range 27.5-32.5)	76
3	35 (FFS range 32.5-37.5)	88
4	40 (FFS range 37.5-42.5)	82
5	45 (FFS range 42.5-47.5)	91
6	50 (FFS range 47.5-52.5)	163
7	55 (FFS range 52.5-57.5)	161
8	60 (FFS range 57.5-62.5)	98
9	65 (FFS range 62.5-67.5)	162
10	70 (FFS range 67.5-72.5)	181
Total		1151

Table S2: Number of rainfall events encountered by the selected 1,151 TMCs, categorized based on rainfall intensity and speed classes. 95% of the times, the encountered rainfall event has intensity between 0-5mm/hr.

Rain (mm/hr)	Speed class (mph)									
	25	30	35	40	45	50	55	60	65	70
>7.5	490	919	1,174	968	1,224	2,682	2,208	2,114	3,520	4,544
5-7.5	533	971	1,219	1,041	1,350	2,588	2,208	2,119	3,467	4,607
2.5-5	1,256	2,359	2,929	2,776	3,448	6,864	5,673	5,169	9,048	11,906
>0-2.5	16,696	30,836	37,354	35,736	44,385	87,793	73,951	68,331	119,637	154,824

Table S3: Number of rainfall events encountered by selected 1,151 TMCs, categorized based on different categories of rainfall intensities and speed classes.

Rain (mm/hr)	Speed class (mph)									
	25	30	35	40	45	50	55	60	65	70
>3	1,857	3,496	4,386	3,954	5,004	10,008	8,354	7,801	13,322	17,403
2-3	848	1,610	1,977	1,808	2,284	4,498	4,009	3,453	6,210	8,296
1-2	1,904	3,252	3,973	3,924	4,996	9,778	8,335	7,343	12,814	16,816
>0-1	14,366	26,727	32,340	30,835	38,123	75,643	63,342	59,136	103,326	133,366

Table S4: Rainfall intensities corresponding to 1st, 2nd, and 3rd quartile for different speed classes

Rain (mm/hr)	Speed class (mph)									
	25	30	35	40	45	50	55	60	65	70
Q3	0.9582	0.9249	0.946	0.9312	0.9559	0.9496	0.9752	0.928	0.9272	0.9456
Q2	0.2104	0.1996	0.2004	0.2024	0.1992	0.2024	0.2136	0.1944	0.1992	0.2008
Q1	0.032	0.0328	0.032	0.032	0.0312	0.0312	0.034	0.0312	0.0304	0.0328